International Guadiana basin Hydrologic modeling using MOHID-Land

Nélson Canuto
nelsonlncanuto@tecnico.ulisboa.pt

Instituto Superior Técnico, Lisboa, Portugal

Março 2019

Abstract

The Guadiana hydrological basin is located in the Iberia Peninsula presenting a dry temperate climate in almost all of its extension with high risk of water scarcity in dry years. It is necessary for the management of the water resources to be aware of the needs that population, agriculture, industry and river ecology have when there is less water available. The environmental modeling is an indispensable tool for the water managers since it allows different climate trends and water consumptions to be analyzed in order to identify less resilient locations. The main objective of this work is to simulate the water dynamics in the Guadiana hydrological basin by applying the MOHID-Land mathematical model. The simulation runs between 1979 and 2014, by simulating the main processes of the water cycle that occur in the basin, such as the surface runoff, the evapotranspiration, the water stored in the soil, in aquifer, and in reservoirs with capacity higher than 10 hm^3. The calibration and validation of the model were done by analyzing several statistical parameters that compare the flows recorded in the hydrometric stations present along the basin. The calibration period had a duration of 10 years, between 1985 and 1995, while the validation occurred between 1995 and 2014. From the results of the calibration and validation of the model there were noticed differences between the hydrometric stations with and without reservoirs influence as well as differences in the results obtained in the Portuguese and Spanish stations, with last one having higher drainage areas.

Key words: MOHID-Land; Guadiana; Hydrologic modeling; Hydrographic basin; Water balance.

1. Introduction

The planning and management of water resources can be defined as instruments used in the regulation and protection of water resources in accordance with the legislation. The water framework directive (200/60/CE) warns of the need to reevaluate river basin management plans in order to prioritize environmental requirements against socio-economic needs. The amount of water on the Earth is quite high, approximately 1,386,000,000 km^3 [1], but only a tiny part of it is freshwater, approximately 2.53% [1] and most of it is located in places of difficult extraction [1]. By 2050, water needs for society are expected to increase by around 55%, compared to the present, due to increases on energy production, household consumption and industrial consumption [2]. If the current water consumption standards are not changed, it is expected that by 2030 there will be a global drinking water deficit of 40% [3]. On Earth, the climate change occurs naturally since its formations, but after the industrial revolution, the anthropogenic activities have introduced changes to this process, and an increase in extreme weather events have been anticipated [4]. With the increase of the global average temperature is expected an acceleration in the water cycle [5], leading to a change in the frequency and intensity of precipitation [6]. The temperature and precipitation changes have a high impact on the rest of the terrestrial water cycle, namely, the surface runoff, the evapotranspiration, the groundwater runoff, and soil moisture [7]. The regions characterized as arid, semi-arid or wetland climates have high vulnerability to changes that increase the risk of desertification [8].

An indispensable tool for the decision-making process of the river basin management plans is the analysis of results obtained in hydrological models. A hydrological model is defined as a simplified representation of the real world, being used to understand and predict the behavior of the various hydrological processes that occur in a basin through the various parameters that define it [9]. The model used, MOHID-Land, is a spatially distributed, continuous, variable time step, physical model developed to model hydrographic basins and aquifers [10].

Objectives

In this work, will be developed a hydrological model for the Guadiana basin to simulate the water dynamics that occur in the basin, using the atmospheric records above the ground (precipitation, air temperature, wind velocity and modulus, solar radiation and relative humidity) [11], the effluent flow rate of reservoirs with a capacity higher than 10 hm^3 [12][13]. The flow obtained in the drainage network in the simulation is compared with the flow recorded by the hydrometric stations [12][13], with the results between 1985 and 1995 used for calibration and in the period between 1995 and 2014 used for validation.

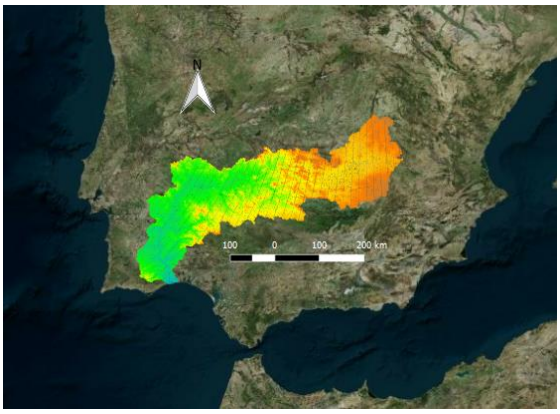

Figure 1 – Geographic location of Guadiana basin.

2. Methodology

2.1. Study area

The study area is located in the Iberian Peninsula, in both Portuguese and Spanish territory, Figure 1. It has a drainage area of 67,133 km^2, of which 55,513 km^2 belong to Spanish territory. Its main river, Guadiana, has it spring located in the Lagoas de Ruidera in Spain at an altitude of 868 m and travels a distance of approximately 860 km until its river mouth between Vila Real de Santo António and Ayamonte in the Gulf of Cádiz [15]. The population living in the basin amounts to 1.9 million inhabitants and the entities responsible for the water resources management are the Agência Portuguesa do Ambiente (APA) [16] and the Confederacíon Hidrográfica del Guadiana (CHG) [17].

The soil type with the most cover in the Guadiana basin are Regosols, occupying a total of 44.03% of the basin area, followed by the Cambisols and Luvisols, with 28.25% and 13.99% respectively. The remaining soils types in basin, Leptosols, Acrisols, Fluvisols, Vertisols, Planosols, Arenosols and Solonchaks, have each less than 5% representativeness [18].

Relatively to the types of land cover in the basin, 64.8% of the area is covered by agricultural practices, 2.9% is covered by evergreen trees, 2.7% is covered by deciduous trees and 12.3% is covered by mixed leaves trees. There are also herbaceous cover (0.1%), shrubs cover (16.4%), water bodies (0.7%) and urban areas (0.1%) [19].

According to the Köppen-Geiger climatic classification, in the basin is found the dry summer temperate climate (Csa) [20] and the cold dry steppe climate (BSk) [20]. The average annual temperature in the basin is 16 ºC, with a mean temperature of 9 ºC in January and 26 ºC in August [21]. The precipitation in the basin isn't evenly distributed, with a weighted average precipitation of 550 mm [21]. The average radiation in the basin varies between 4.68 $kwh.dia.m^{-2}$ and 5.20 68 $kwh.dia.m^{-2}$ [22].

In the Guadiana basin there are a total of 39 reservoirs with storage capacity higher than 10 hm^3 and in operation before 2011[12][13].

2.2. MOHID Model

The model used in this work was developed at MARETEC (Marine and Environmental Technology Research Center) and his main propose is to simulated the various physical and biochemical processes that occur in costal and oceanic areas, in estuaries, watersheds and aquifers [23].

For simulating in watersheds and aquifers, MOHID-Land, simulates the movement of water in the runoff through the St Venant equation (1) in 2D and in the drainage network through the St Venant equation (1) in 1D [10].

$$\frac{\partial v_i}{\partial t} + v_j \frac{\partial v_i}{\partial x_j} = -g\left(\frac{\partial H}{\partial x_i} + S_{fi}\right) \qquad (1)$$

The St Venant equation indicates that the partial derivatives of flow velocity equal to the hydraulic gradient, gravity force and the water surface slope. By multiplying both members of the equation with vertical area yields the flow rates.

The surface slope is defined by the Manning-Strickler´s empirical law(S_{fi})[10], where (R_h) is the hydraulic radius (defined by the quotient of the wet cross-section and the wet perimeter), the roughness coefficient of Manning (m_n), as can be seen in the equation (2).

$$\left(S_f\right)_i = \frac{{m_n}^2 |Q| Q_i}{A^2 R_h^{\frac{4}{3}}} \qquad (2)$$

The flow in the satured and unsatured zones of the soil is calculated using the Richards equation (3)[10].

$$\frac{\partial \theta}{\partial t} = \frac{\partial}{\partial x_i}\left(\phi_{H_2O}\right) = \frac{\partial}{\partial x_i}\left(-K\left(\frac{\partial H}{\partial x_i}\right)\right) \qquad (3)$$

The Richards equation indicated that the soil moisture variation over time corresponds to the hydraulic gradient $(\frac{\partial H}{\partial x_i})$ and soil conductivity (K) derivated in order of space. The soil water conductivity (K) is calculated using Mualem-model

(4), using the saturated conductivity (Ks), effective cell saturation (SE), empirical coefficient of pore connectivity (L) and the (m) coefficient, obtained in equation (5), which depends on the pore size distribution (n).

$$K = K_s \times S_E^L \times \left(1 - \left(1 - S_E^{\frac{1}{m}}\right)^m\right)^2 \quad (4)$$

$$m = 1 - \frac{1}{n} \quad (5)$$

The water flow between the soil and the atmosphere is calculated in the model by using the reference evapotranspiration equation (6), from the FAO Penman-Montheith method [10].

$$ET_o = \frac{0.408\Delta(R - G) + \left(\gamma \frac{900}{T + 273} U_2 (e_s - e_a)\right)}{\Delta + \gamma(1 + 0.34u_2)} \quad (6)$$

The calculation of the reference evapotranspiration is performed using the vapor pressure curve (Δ), surface net radiation (R), soil heat flux (G), psychrometric constant (γ), temperature (T), the wind speed at 2 meters height from the ground (U_2), the water vapor pressure (e_a) and the saturation vapor pressure (e_s).

The reference evapotranspiration is the used to calculate the potential evapotranspiration (7) [10], which also depends on the vegetation coefficient(K_c).

$$ETP = K_c \times ET_o \quad (7)$$

The calculation of soil moisture (θ) is made through the water retention curve given by the Van Genuchten model (8)[33]. In this equation (α) corresponds to the inverse value of the air inlet, (h) is the effective pressure, (θ_r) is the residual water content in the soil and the (θ_s) is to the soil water content at saturation.

$$\theta = \theta_r + \frac{\theta_s - \theta_r}{[1 + (\alpha|h|)^n]^{1-\frac{1}{n}}} \quad (8)$$

The water flow between the cells of the soil surface and the runoff is calculated by the Curve number (CN). This parameter influences the empirical equation (9) that related the surface flow (Q) with the precipitation (P), the maximum water retention capacity in the soil (S) and the precipitation losses due to vegetation cover, infiltration and water retention(I_a). The maximum water retention capacity in the soil (S) is related with the curve number (CN) through the equation (10). The curve number (CN) varies between 30 and 100.

$$Q = \begin{cases} 0 & , se\ P \leq I_a \\ \left(\frac{(P - I_a)^2}{P - I_a + S}\right) & , se\ P > I_a \end{cases} \quad (9)$$

$$S = \frac{25400}{CN} - 254 \quad (10)$$

Model implementation

In the implementation of the model, a two-dimensional mesh was developed, having 5 km x 5 km cell size, and located between the coordinates (8º13'58,8''W ; 37º7'40,44''N) and (2º6'27''W ; 40º30'21,24'' N).

Using the two-dimensional mesh and a digital terrain model (Copernicus Land monitoring Service EU-DEM) [24] with 1 km resolution was obtained the digital terrain model (DTM) used in the model by interpolation. The existing depression in the DTM were removed because the MOHID-Land does not allow the existence of depressions within the basin. Through the DTM and the location of the basin mouth, the delineation, the geometry and the drainage network of the basin were obtained. The dimensions of the drainage network cross section in the surface [25] and the bottom [26] according to its drainage area were implemented.

The soil layer implemented in the model was obtained using the DTM and stipulating a minimum thickness of 0.3 m and a maximum thickness of 30 m, starting from a maximum slope of 1. At the initial time of the simulation was stipulated that 83% of the soil was saturated. Through the interpolation of the harmonized World Soil Database at 1: 1,000,000 scale [18] and the DTM, the file containing each soil type existing in each cell in the model was obtained, with the Solonchak soil not represented in the model. For each type of soil, the curve number (CN), saturated soil conductivity(K_s), saturated soil water retention (θ_s), residual water retention(θ_r), the inverse of air inlet (α), the pore size distribution (n) and the empirical connectivity of pores (L)[27] [34].

Interpolating the DTM with GLC 2000 at 1:1 000 00 scale [19] was obtained the land cover to be implemented in the model, with the urban areas having no representation. For each land cover was defined a vegetation coefficient (K_c)[28] and a Manning coefficient (Mn)[29].

The atmospheric data used in the model were provided by the SAFRAN system and interpolated with the mesh used in the project. SAFRAN is a model that estimates the atmospheric variables in climatically homogeneous zones through values observed every 6 hours, interpolating in hourly data. From the SAFRAN was used data on precipitation, relative humidity, wind modulus, air temperature and solar radiation [11].

In Guadiana basin there are 39 reservoirs with capacity higher than 10 hm^3 in operation between 1979 and 2012. Of the 39 reservoirs, 11 began operating before the start of the simulation and the remaining reservoirs were built and started operating during the years of simulation [12][13].

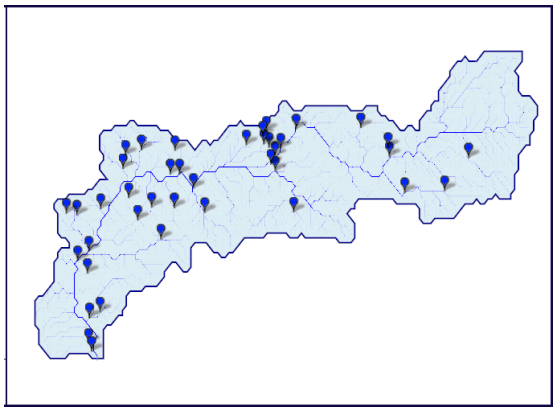

Figure 2 – Reservoirs location in the Guadiana basin.

To implement the reservoirs in the model it was necessary data regarding its location, the minimum and maximum volume storage and its accumulation curve. When there is available data of discharge flow rates, it was implemented in the model, otherwise an operation curve was implemented to determine the discharge flow rate of the reservoir. In the start of the simulation, the reservoirs already in operation were implemented in October 1, 1979 with 45% of their maximum volume occupied with water.

In order to perform the calibration and validation of the model, it was necessary to obtain tools that allow the comparison of the obtained flow in the drainage network in the simulation and the observations in the hydrometric stations. It was selected the hydrometric stations with a minimum of 5 years of data in the calibration period, figure 3 [13][14].

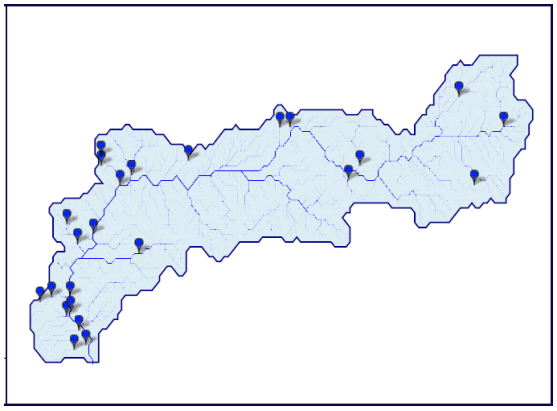

Figure 3 –Hydrometric stations location in the Guadiana basin.

2.3. Statistical tools

It is used 4 different statistical coefficients to analyze the similarity between the flow data from the hydrometric stations and the correspondent flow in the simulation. The NSE (Nash-Sutcliffe efficiency) is utilized to determine the relative magnitude of the residual variance between the simulated values and the observed data (11) [30]. Ideally its value is 1.

$$NSE = 1 - \left[\frac{\sum_{i=1}^{n}(Y_i^{obs} - Y_i^{sim})^2}{\sum_{i=1}^{n}(Y_i^{obs} - Y^{médio})^2}\right] \qquad (11)$$

The determination coefficient (R^2) (12), describes in percentage the capacity of the simulation to explain the variability in the observations, and there is a perfect relation when its value is 1. [30][31]

$$R^2 = \left[\frac{\sum_{i=1}^{n}(Y_i^{obs} - Y^{\overline{obs}})(Y_i^{sim} - Y^{\overline{sim}})}{\left[\sum_{i=1}^{n}(Y_i^{obs} - Y^{\overline{obs}})^2\right]^{0.5}\left[\sum_{i=1}^{n}(Y_i^{sim} - Y^{\overline{sim}})^2\right]^{0.5}}\right]^2 \qquad (12)$$

The NRMSE coefficient (Normalized root mean square error) (13) is used to evaluate the accuracy of the model. It normalization allows it to be independent of the units and scale of the parameter to be analyzed [30]. The closer to zero it is, the better the approximation of the simulation data to the hydrologic stations data.

$$NRMSE = \frac{\sqrt{\frac{\sum_{i=1}^{n}(Y_i^{obs} - Y_i^{sim})^2}{n-1}}}{\sqrt{\sum_{i=1}^{n}(Y_i^{obs} - Y_i^{\overline{obs}})^2}} \qquad (13)$$

PBIAS (Percent bias) (14) is used to verify if the simulation is overestimating or underestimating the results compared to the observed values. This coefficient is a percentage, indicating an overestimation when its value is negative and an underestimation when its value is positive. Ideally it has a value of zero [30].

$$PBIAS = 100 \times \left[\frac{\sum_{i=1}^{n}(Y_i^{obs} - Y_i^{sim})}{\sum_{i=1}^{n}(Y_i^{obs})}\right] \qquad (14)$$

In the Table 1 is indicated the range values of each statistical parameter used to classify the differences between the hydrometric stations data flow and the simulation drainage network flow data.

Table 1 – Statistical coefficients classification.

	Good	Satisfactory	Poor
NSE	[0,75; 1]	[0,5; 0,75]	[-∞; 0,5]
R^2	[0,75; 1]	[0,5; 0,75]	[0; 0,5]
RMSE	[0; 0,5]	[0,5; 0,7]	[0,7; +∞]
PBIAS	±[0%;10%]	±[10%;25%]	±[25%;inf]

In the addition to the quantitative analysis provided by the statistical coefficients, the permanence flow is used to compare the flows qualitatively. The permanence flow is a useful tool to analyze the flow without considering the time variation of the given data. The flows are order according to their magnitude and for each flow is associated with a frequency of occurrence, with higher flows having lowers probabilities of happening.

3. Calibration

3.1. Parameters

The model simulation was initialized on October 1, 1979, and the calibration period was defined between October 1, 1985 and September 30, 1985. The initial 6 years were used as a buffer time for the model to stabilize. The main parameters of the model that were modified in the calibration were the curve number (CN), Manning coefficient (Mn), vegetation coefficient (Kc) and soil saturation conductivity (Ks).

The drainage network dimensions where modified, as can be seen in table 2. This change was necessary to allow the flow in certain places to occur in periods of critical precipitation by accumulation of high volumes of water in some cells.

Table 2 – Cross sections dimensions before and after calibration.

Drainage Area (km^2)	Width at surface (m)	
	Initial	Final
18	3.50	6.10
25	3.80	7.40
100	6.70	21.30
1,000	23.00	60.80
10,000	79.00	138.20
67,000	300.00	358.00

The modifications made during the calibration to the soil proprieties, specifically the curve number (CN) and soil saturation conductivity (Ks) are defined in table 3. The curve number (CN) influences the rate of infiltration of water into the soil and its increase corresponds to a decrease in the water infiltration capacity in the soil increasing the runoff and in its turn, the flow in the drainage network.

The saturated soil conductivity (Ks) corresponds to the vertical flow velocity that can occur in the soil until saturation if reached. Its increase implies a higher flow rate in the drainage network because it allows a higher infiltration rate at water table level, which is in equilibrium with the drainage network. In situations with low flow velocity and having the same infiltration rate, can occur saturation in the soil upper layers and the flow to the drainage network will be mainly superficial runoff.

Table 3 – Soil type parameters before and after calibration.

Soil Type	Curve number **CN** (-)		Saturated soil conductivity **Ks** (cm/day)	
	Initial	Final	Initial	Final
Regosols	85	79	60	200
Arenosols	84	77	60	550
Cambisols	76	69	60	70
Fluvisols	71	71	12	22
Leptosols	89	79	12	18
Luvisols	66	66	60	85
Planosols	74	74	60	85
Acrisols	65	68	60	85
Vertisols	70	70	25	6

The table 4 shows the changes made to the parameters related to the land use, namely, the Manning coefficient (Mn) and the vegetation coefficient (Kc).

The manning coefficient (Mn) represents the resistance of the surface to the water flow. The increase of this parameter implies the increase in the resistance of to the surface flow and consequently, the decrease of the flow rate in the drainage network after the precipitation and an increase of the flow after the maximum flow peak.

The vegetation coefficient (Kc) é is used to calculate the evapotranspiration. Its increase is reflected in the increase of water consumption by the plant, reducing the amount of water in the soil and influencing the infiltration of the water into the soil.

Table 4 – Land use parameters before and after calibration.

Land use	Manning Coefficient Mn [$s.m^{-1/3}$]		Vegetation coefficient Kc [-]	
	Initial	Final	Initial	Final
Agriculture practices	0.045	0.043	0.92	0.96
Mix leaves trees	0.227	0.225	0.95	0.85
Evergreen trees	0.125	0.127	1.07	1.00
Deciduous trees	0.125	0.230	0.80	0.80
Herbaceous plants	0.039	0.039	0.85	0.85
Shrubs	0.057	0.058	0.90	0.90
Water bodies	0.032	0.035	0.00	0.00

3.2. Hydrometric stations

The model calibration started with the qualitative analysis of the permanence flow in the hydrographic stations and their corresponding location in the model. Among the analyzed stations, Amieira presents one of the best calibrations results. Located in central Alentejo, until 1995 it is not influenced by any reservoir with a capacity greater than 10 hm^3. In the permanence flow, figure 4, it is verified that the both curves have the same tendency and similar values, except in the frequency ranges with probably of exceedance lesser then 4%, with the simulation registering lower values. Among the stations that present a calibration with worse results, the station 4214, located in the region of Ciudad Real, registers a higher flow in the drainage network of the simulation than in the hydrometric station, for all frequencies of exceedance, figure 5.

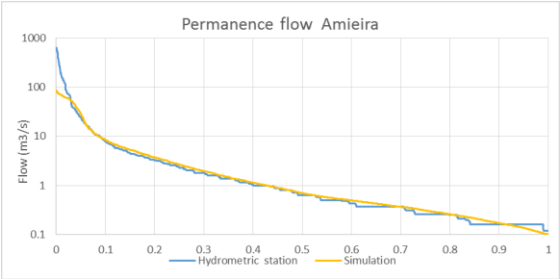

Figure 4 - Permanence curve for Amieira station in calibration period.

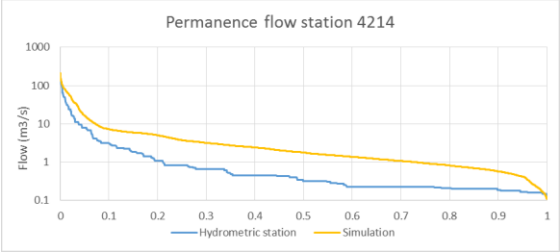

Figure 5 – Permanence curve for 4214 station in calibration period.

The qualitative results verified for Amieira and 4214 stations are corroborated by their quantitative evaluation, using the statistical parameters, table 5.

Table 5 – Statistical coefficients for Amieira and 4214 stations in calibration period.

Station	Amieira	4214
Years with data	8.9	6.0
Station mean flow	4.287	1.490
Simulation mean flow	4.005	5.191
NSE	0.707	-1.345
R^2	0.868	0.645
NRMSE	0.053	0.182
PBIAS	6.584	-248.290

It is verified that the Amieira station has an NSE of 0.707, which corresponds to the relative magnitude of the variance between the simulated values and the observed data, being a satisfactory result. The R^2 is 0.868, which corresponds to a good capacity of the simulation to explain the variability of the observed data. The NRMSE has the value of 0.053, a good value for the evaluation of the accuracy of the model. The PBIAS is 6,584%, which corresponds to a good low overestimation of the flow. Regarding the results obtained for the 4214 station, only the NMRSE coefficient have a good value, 0.182. The R^2 obtain was 0.645, indicating a satisfactory explanation of the simulation to the variability in the hydrometric station data. In the PBIAS analysis it is verified that there is an overestimation of the flow, in the order of 248.29%. The overflow is also verified in the relative magnitude of the variation, with an NSE of -1,345.

Globally 7 stations have good values in the NSE coefficient, 4 have a satisfactory NSE and 13 have a poor NSE coefficient, figure 6.

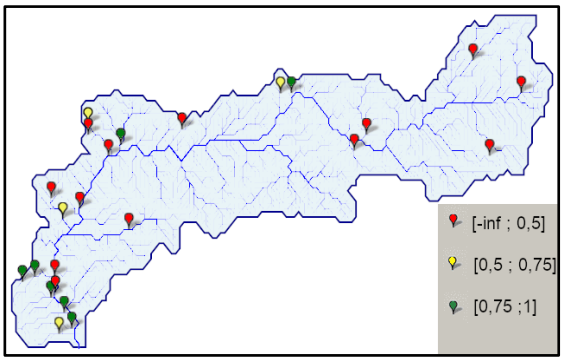

Figure 6 – NSE results for different stations in the calibration period.

Regardless the R^2, a total of 14 stations have a good value, corresponding to a simulation with a good explanation of the observation variability, 5 have satisfactory values and 4 got poor results, as we can see in figure 7.

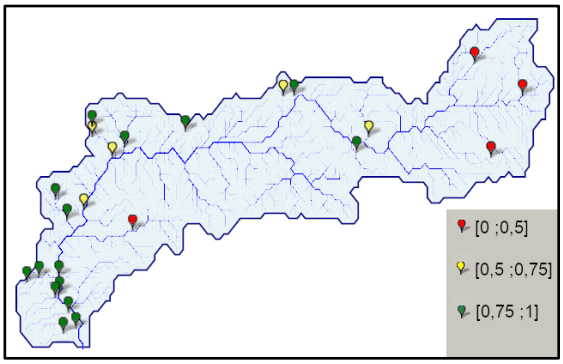

Figure 7 – R^2 results for different stations in the calibration period.

The NRMSE coefficient have the best results of all statistical parameters in the calibration, with 19 of 24 stations having good results. The remaining stations have poor results, as can be seen in figure 8.

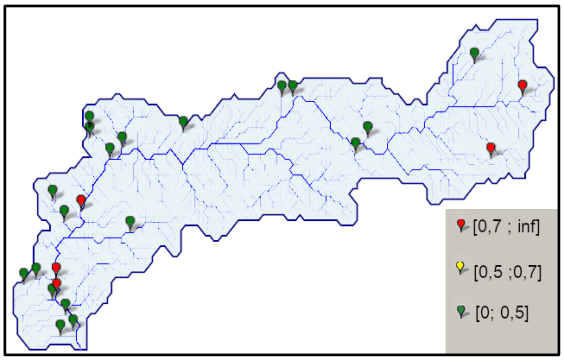

Figure 8 - NRMSE results for different stations in the calibration period.

The last coefficient, PBIAS, it can be seen in figure 9. From the 6 stations that have a good result, with half of them with overestimations and the other half with underestimation. 3 stations have satisfactory overestimation and one with a satisfactory underestimation results. The other 13 stations have poor results with just one of them having underestimation.

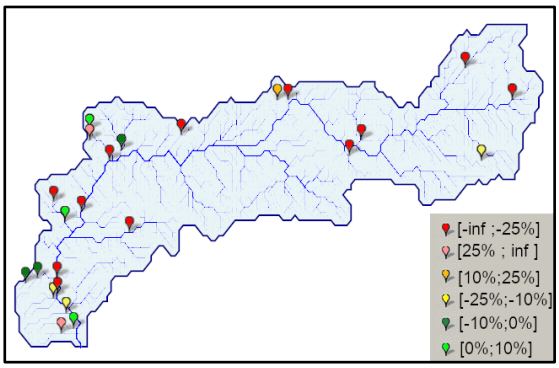

Figure 9 - PBIAS results for different stations in the calibration period.

In figure 10 is the global analysis of all statistical parameters during the calibration for the 24 stations implemented in the model. There is a total of 4 stations with all of statistical parameters having good results. With a little worse results, 5 stations have at least one statistical coefficient with satisfactory results. The remaining 15 stations have at least one statistical coefficient non acceptable.

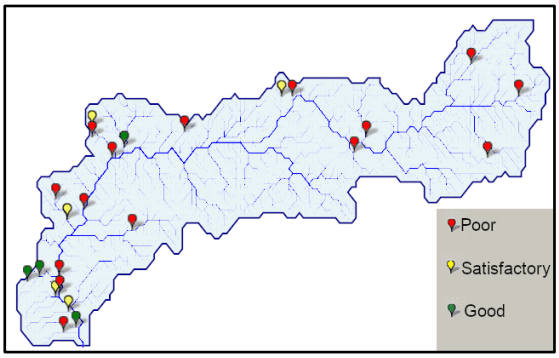

Figure 10 - Overall results for different stations in the calibration period.

4. Validation

4.1. Hydrometric stations

In the validation period (1995-2014) were considered just 19 of the 24 stations used in calibration. The remaining 5 stations have less than 3.5 years of flow data records in the validation period.

The Amieira station, which in calibration period was no influenced by a reservoir, from 1998 onwards is influenced by Monte Branco dam. In the analysis of his permanence flow curves, figure 11, it is verified that only for frequencies of exceedance with less than 5% probability, the simulation has a difference in the flows tendency, with lower flows. In the remaining frequencies, the simulation permanence flow is slightly higher than in the hydrometric station, but with very similar values for each frequency of exceedance. In the 4214 Station, figure 12, for the frequencies of exceedance with a probability lower than 2%, both simulation and hydrometric station have similar flows. In the remaining frequencies of exceedance, the simulation flow is always higher than in the hydrometric station, but comparably to the calibration results the differences between flows are lower.

Regarding the statistical coefficients, table 6, in the Amieira Station there is an improvement of the NSE, changing from satisfactory to good coefficient, 0.788. The R^2 shows a slightly worse result, 0.788, but remains a good coefficient. In the NRMSE there is virtually no changes and the PBIAS is also very similar, with an underestimation of 6.584%. In the 4214 station, the PBIAS have a poor result, -62.831%, but it is well below the calibration value, -248.29%. The NSE and R^2 are both satisfactory, 0.684 and 0.716 respectively. The NRMSE improved, changing from 0.182 to 0,042.

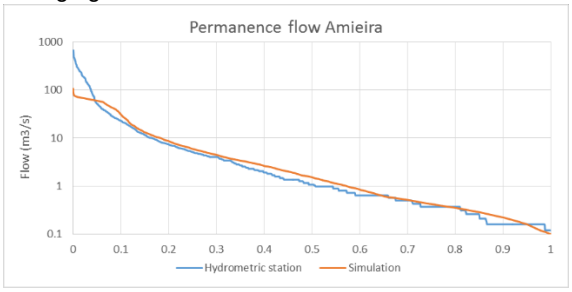

Figure 11 - Permanence curve for Amieira station in validation period.

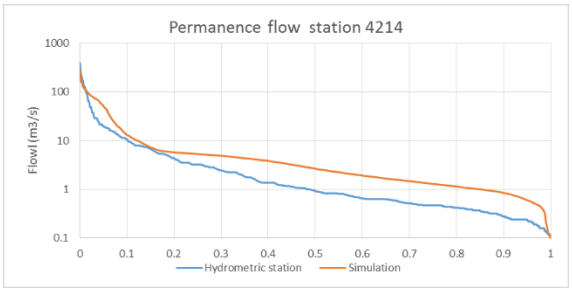

Figure 12 - Permanence curve for 4214 station in validation period.

Tabela 1 - Coeficientes estatísticos nas estações da Amieira e 4201.

Station	Amieira	4214
Years with data	6.1	16.0
Station mean flow	9.300	5.374
Simulation mean flow	8.653	8.750
NSE	0.788	0.648
R^2	0.820	0.716
NRMSE	0.054	0.042
PBIAS	6.955	-62.831

Overall, figure 13, in the validation period there are 4 stations with a good NSE coefficient, 5 stations have a satisfactory NSE coefficient and 10 stations have a poor NSE coefficient.

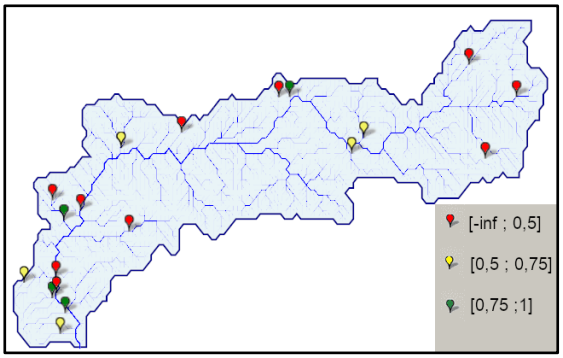

Figure 13 - NSE results for different stations in the validation period.

For the R^2 coefficient, figure 14, a total of 8 stations have a good result, 5 of them have satisfactory values and the remaining 6 stations have a poor performance in this statistical parameter.

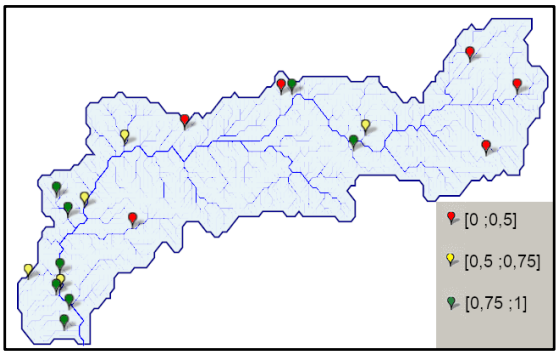

Figure 14 – R^2 results for different stations in the validation period.

For NRMSE coefficient, figure 15, a total of 16 stations show a good accuracy of the model flow and just 3 stations have a poor result.

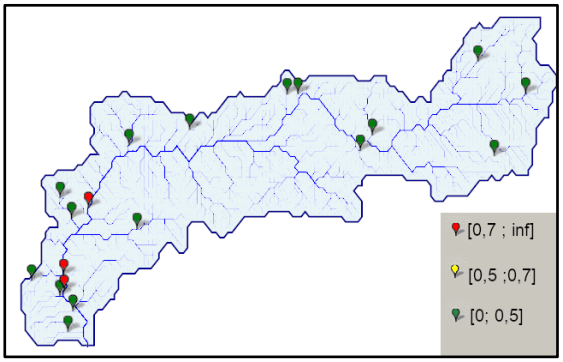

Figure 15 - NRMSE results for different stations in the validation period.

The PBIAS coefficient, figure 16, show that 4 stations have a good estimation of the flow in the validation period. One station has a satisfactory PBIAS coefficient and the remaining 14 stations have poor results, with 11 of them with overestimation.

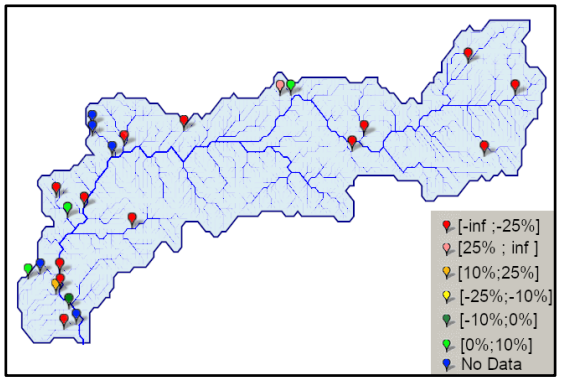

Figure 16 - PBIAS results for different stations in the validation period.

In the Overall analysis if all statistical coefficients in the validation period, figure 17, it can be seen that 3 stations have good results in all parameters, 2 stations have a satisfactory result and 14 stations have at least one statistical parameter with poor results. The remaning 5 stations that were used in the calibration cannot be validated.

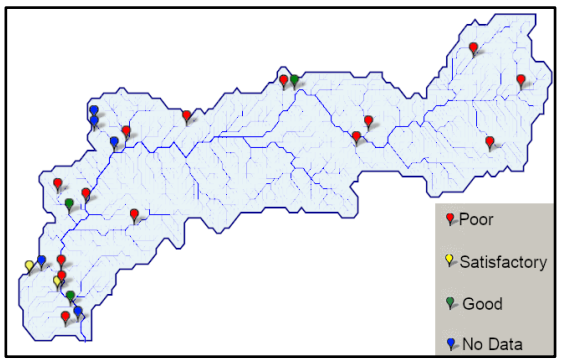

Figure 17 - Overall results for different stations in the validation period.

Discussion

In the validation period there was a decrease of stations with good results, going from 4 to 3 stations. Of those 4 stations with good calibration coefficients, 2 of them do not have enough data to be validated (Monte da Ponte and Tenência), the Entradas station changes from a good calibration to a satisfactory calibration because of the NSE, and the 4255 station have a poor validation, influenced by a PBIAS of 33.68%, influences of the reservoir constructed in 1996, Villar del Rey. From stations with a satisfactory calibration, Monte Pisão doesn't have enough data in the validation period, Oeiras keeps the same global coefficients results and the Amieira station goes from a satisfactory calibration to a good validation. In the 4218 station, 3 of 4 statistical coefficients gets poor results, namely, NSE, R^2 and PBIAS. From the stations with poor calibration, Monte da Vinha do not has enough data to be validated, the 4212 station improves and gets a good validation, and the remaining stations keep their statistical coefficients not acceptable. It should be noted that the stations with poor validation and calibration, 8 of them

presented a significant improvement, mainly in PBIAS, but not enough for satisfactory results.

It is verified that in both calibration and validation periods, that the model has better results in the Portuguese territory of the basin, especially in the stations without influence of the reservoirs. In the upstream area of the basin, the first hydrometrical stations have almost all statistical coefficients with poor results, both in calibration and in validation periods. A plausible reason is the type and use of existing soil in its drainage area, composed of very permeable limestone soils and with larges extensions of agricultural fields, with overexploitation of aquifers [32], a factor that the model cannot simulate. The stations with influence of reservoirs have the worse statistical coefficients, most of them located downstream of the reservoirs of the Guadiana river that are influenced by the excess flow from their tributaries upstream river basins.

The implementation of reservoirs is crucial in basin modeling, allowing to storage huge volumes of water that otherwise would flow on the drainage network until the basin mouth in simulation after the precipitation, not corresponding to the reality. The reservoirs that doesn't have data on their discharges need to be implemented with an operation curve that allows to simulate different discharges rules in different times of the year.

Conclusion

This model allows to simulate the water balance with satisfactory results in several points of the basin, mainly in locations with smaller drainage areas and in Portuguese territory. The majority of hydrometric stations in the basin that have high drainage areas and the stations with reservoir influence obtained unsatisfactory results, with several reservoirs without any data regarding their discharges.

For future works, it is suggested to modify MOHID-Land in relation to the discharge flow of the reservoir when there is no data available, with the possibility to apply different rules to define of the operation curve of the reservoir discharge, obtaining a more realistic approximation of discharges in different times of the year, with the population and the ecological flow having different water needs in the winter and in the summer. Changes in the soil layer thickness, in Manning coefficient, in the curve number at the basin drainage areas that had the worse results and the implementation of reservoirs with smaller capacity, may allow to diminish the drainage network flow right after precipitation and to increase the flow in the remaining time and improve the simulation results and have better statistical coefficients.

References

[1] Gleick, P.H.(1993). *Water in Crisis: A Guide to the World's FreshWater Resources*. New York: Oxford University Press.

[2] UNWATER. (2015). *The United Nations World Water Development Report 2015*. Paris: United Nations Educational, Scientific and Cultural.

[3] 2030 WRG. (2009). *Charting our water future: Economic frameworks to inform decision-making.* Washington DC: 2030 WRG

[4] Ripple, W. J., Wolf, C., Newsome, T. M., Galetti, M., Alamgir, M., Crist, E., Laurance, W. F. (2017). *World Scientists' Warning to Humanity: A Second Notice*. *BioScience*, 1026-1028.

[5] Oki, T., & Kanae, S. (2006). *Global Hydrological Cycles and World Water Resources. FreshWater Resources*, 1068-1072.

[6] Trenberth, K. E., Dai, A. O., Rasmussen, R. Y., & Parsons, D. B. (2003). *THE CHANGING CHARACTER. AMERICAN METEOROLOGICAL SOCIETY*, 1205-1217.

[7] Milly, P. C., Arnold, J. G., Liew, M. W., Bingner, R. L., Harmel, R. D., Veith, T. L. (2007) MODEL EVALUATION GUIDELINES FOR SYSTEMATIC QUANTIFICATION OF ACCYRACY IN WATERSHED SIMULATIONS. *American Society of Agricultural and Biological Engineers*, 885-900.

[8] Tombolini, I., Colantoni, A., Renzi, G., Sateriano, A., Sabbi, A., Morrow, N., & Salvatia, L. (2016). *Lost in convergence, found in vulnerability: A spatially-dynamic model for desertification risk assessment in Mediterranean agro-forest districts*. *Elsevier*, 971-981.

[9] Gayathri, K. D., Ganasri, B. P., & Dwarakish, G. P. (2015) *A Review on Hydrological Models. Aquatic Procedia*, 1001-1007.

[10] MARETEC. (2018). MOHID. Retrieved from What is MOHID?: http://www.mohid.com/pages/home/whatismohid.shtml

[11] Quintana-Seguí, P.T.-M.(2017). Validation of a new SAFRAN-based gridded precipitation product for Spain and comparations to Spain02 and ERA-Interim, Hydrol. Obtido de https://doi.org/10.5194/hess-21-2187-2017

[12] SNIRH. (2018). Sistema Nacional de Informação de Recursos Hídricos. Obtido em SNIRH: http://snirh.apambiente.pt/

[13] CEH-CEDEX. (2018). *CENTRO DE ESTUDIOS HIDROGRÁFICOS*.
Retrieved from CENTRO DE ESTUDIOS Y EXPERIMENTACIÓN DE OBRAS PÚBLICAS:http://ceh-flumen64.cedex.es/anuarioaforos/afo/embalse-mapa_estaciones.asp?gr_cuenca_id=4&resolucion=1920

[14] CEH-CEDEX. (2018). *CENTRO DE ESTUDIOS HIDROGRÁFICOS*. Retrieved from CENTRO DE ESTUDIOS Y EXPERIMENTACIÓN DE OBRAS PÚBLICAS: http://ceh-flumen64.cedex.es/anuarioaforos/afo/estaf-cdr_datos.asp?gr_cuenca_id=4

[15] CADC. (2018). Documento de coordenação elaborado durante o processo de planeamento 2016-2021 para as bacias hidrográficas internacionais partilhadas por Espanha e Portugal. Obtido em: https://apambiente.pt

[16] APA. (2018). Agência Portuguesa do Ambiente-Atribuições. Obtain at APA: https://www.apambiente.pt/index.php?ref=5&subref=634

[17] CHG. (2018). Comisaría de Aguas. Obtido em Confederacíon Hidrográfica del Guadiana: https://www.chguadiana.es/el-organismo/estructura-y-funciones/comisaria-de-aguas

[18] ESDAC. (2001). EUROPEAN SOIL DATA CENTER. Obtido de European Soil Database v2.0 :https://esdac.jrc.ec.europa.eu/resource-type/datasets

[19] Joint Research Centre (2018)Joint Research Centre obtido do The European Commision's science and knowledge service em: https://forobs.jrc.ec.europa/products/glc2000/products.php

[20] IPMA, AEMET. (2010) Atlás Climático Ibérico.em: http://www.ipma.pt/resources.www/docs_pontuais/ocorrencias/2011/atlas_clima_iberico.pdf

[21] CADC. (2014) Comissão para a aplicação e o desenvolvimento da Convenção de Albufeira obtido em: http://www.cadc-albufeira.eu/pt/cuencas-hidrograficas/cuenca-guadiana/

[22] Aemet. (2018). Atlas de Radiación Solar en España utilizando datos del SAF de clima de EUMETSAT.

[23] MARETEC. (2018). MOHID. Obtido de What is MOHID?: http://www.mohid.com/pages/home/whatismohid.shtml

[24] European Environmental Agency.(2017).European environmental Agency. Obtido de Copernicus Land Monitoring Service EU-DEM :https://www.eea.europa.eu/data-and-maps/data/Copernicus-land-monitoring-service-eu-dem

[25] Andreadis, K. M., Schumann, G.J.-P., & PAvelsky, T. (2013). A simple global river bankfull width and depth database. Water Resources Research 7164-7168. Obtido em: http://gaia.geosci.uns.edu/rivers/

[26] Neal, J. C., Odoni, N. A., Trigg, M. A., Freer, J. E., Garcia-Pintado, J., Mason, D C., Bates, P. D. (2015). Efficient incorporation of channel cross-section geometry uncertainty into regional and global scale flood inundation models. *Journal of Hydrology*, 169-183.

[27] USDA-SCS. (1972) National Engineering Handbook. Em Section 4. Table 10.1

[28] FAO. (1998) Crop Evapotranspiration. em R. G. Allen, L. S. Pereira, D. Raes, & Smith, *FAO irrigation and drainage Paper nº 56*, obtido em FAO IRRIGATION

[29] Pestana, R., Matias, M., Canelas, R., Araújo, A., Roque, D., Zeller, E.V., Heleno, S. (2013). Calibration of 2D Hydraulic Inundation Models in the floodplain region of the lower Tagus river. ESA Living Planet Symposium. Edinburgh: RIVERSAR.

[30] Moriasi, D. N., Arnold, J. G., Liew, M. W., Bingner, R. L., Harmel, R. D., & Veith, T. L. (2007). MODEL EVALUATION GUIDELINES FOR SYSTEMATIC QUANTIFICATION OF ACCURACY IN WATERSHED SIMULATIONS. *America Society of Agricultural and Biological Engineers,* 885-900.

[31] Legate, D. R., & Jr., G. J. (1999). Evaluating the use of "goodness-of-fit" measures in hydrologic and hydroclimatic model validation. *WATER RESOURCES RESEARCH*, 233-241.

[32] APA. (2016). Plano de Gestão de Região Hidrográfic Parte 2- Caracterozação e diagnóstico. Obtido de Agéncia Portuguesa do Ambiente: http://apambiente.pt/_zdata/Politicas/Agua/PlaneamentoeGestao/PGRH/2016-2021/PTRH7/PGRH7_PArte2.pdf

[33] Van Genuchten, m. T. (1980). A closed from equation for predicting the hydraulic condutctivity of unsatured soils. *Soil Science Society American Journal*, 892-898.

[34] J.H.M, W., A., Nemes, A., & Bas, C. L. (1999). Development and use of a database of hydraulic properties of European soils. *Elsevier*, 169-185.